2020 59th Annual Conference of the
Society of Instrument and Control Engineers of Japan (SICE)
September 23-26, 2020, Chiang Mai, Thailand

Prediction of Wind Speed and Direction using Encoding - forecasting Network with Convolutional Long Short-term Memory

Anggraini Puspita Sari[1†], Hiroshi Suzuki[1], Takahiro Kitajima[1], Takashi Yasuno[1], Dwi Arman Prasetya[2] and Abd. Rabi'[2]

[1]Department of Electrical and Electronic Engineering, Tokushima University, Tokushima, Japan
(Tel: +81-88-656-7458; E-mail: {anggi, kitaji-t}@ee.tokushima-u.ac.jp,
{suzuki.hiroshi, yasuno.takashi}@tokushima-u.ac.jp)
[2]Department of Electrical Engineering, University of Merdeka Malang, Malang, Indonesia
(Tel: +62-813-7380-4888; E-mail: {arman.prasetya, arrabik}@unmer.ac.id)

Abstract: This paper presents the prediction system of wind speed and direction one hour ahead using encoding-forecasting network with convolutional long short-term memory (ConvLSTM). The input of prediction system is wind speed and direction which are represented as image data on the 2D coordinate and provided by Automated Meteorological Data Acquisition System (AMeDAS) in Japan. Performances of the proposed prediction system are evaluated based on root mean square error (RMSE) between observed and predicted value. The goal of the proposed prediction system is to improve prediction accuracy and it is confirmed by comparing the result of the prediction system of four seasons.

Keywords: wind speed, wind direction, LSTM, encoding-forecasting network, ConvLSTM.

1. INTRODUCTION

Renewable energy resources will hold an important role in the future and the target of global electricity generation from renewable energy resources can supply 31% of total world energy demand at 2035[1][2]. Renewable energy resources can decrease dependency on fossil fuel and reduce affects global climate change, health risks, and an adverse impact on the environment[3]. Renewable energy resources have the potential to supply energy services almost zero-emissions of greenhouse gases[1].

Among various kinds of renewable energy, wind power generation is rapidly introduced as an alternative electric power generation and attracted attention on the world. The main problem of wind power generation is the fluctuation of wind speed and direction. If we can predict the output of wind power generation based on the prediction of wind speed and direction, we can offer this information to power companies that can help for the planning operation of the thermal power plant and stabilize the electric power system[4].

The condition of wind speed and direction is unstable in Japan compared with Europe and Americas. It because of complex terrain and the prediction of wind data (wind speed and direction) is also difficult. The main prediction method of wind data are divided into numerical and statistical methods. The numerical methods requires long time processing and many computation costs. The statistical method predicts future data from current and previously observed data[5].

Accordingly, we propose statistical prediction system using the encoding-forecasting network with convolutional long short-term memory (ConvLSTM). Proposed system uses images that represent wind data. The system predicts wind data one hour ahead by considering the ability to adjust pumped-storage hydroelectricity and thermal power plant[6]. The wind data is obtained by AMeDAS at 10 min interval in Tokushima city, Japan.

The several simulations of the proposed prediction system using four seasons which is characteristic of the Japanese climate. The effectiveness of the prediction system verifies by comparing LSTM and ConvLSTM systems each season in one year.

2. RELATED WORKS

At present advances in deep neural networks, especially long short-term memory (LSTM) is popular choices for sequence learning tasks and suitable for end to end learning [7][8]. LSTM is learning based on time-series information, and selective memory. LSTM is a good solution for time sequence data and it is often used to dialogue system and sentence generation.

The ConvLSTM is proposed image prediction which is a combined convolutional neural network (CNN) and LSTM and also uses to solve image sequence. The proposed system using the encoding-forecasting network as an improvement of LSTM and precipitation nowcasting[8][9]. In this paper, we use wind data are plotted to image and use to input ConvLSTM which can solve the sequence to sequence learning process.

3. PROPOSED SYSTEM

3.1. Definition of wind speed and Direction

The wind data of AMeDAS is provided as wind speed and direction. Fig. 1 shows 16 wind directions of AMeDAS. The wind data can be represented on coordinate system as shown in Fig. 2. The direction of east (E) - west (W) accords to X-axis and the direction of north (N) - south (S) accords to Y-axis. X and Y components of wind speed, $v_X(t)$ and $v_Y(t)$ are shown in Eqs. (1)

† Anggraini Puspita Sari is the presenter of this paper.

978-1-7281-1089-9 PR0001/20 ¥400 © 2020 SICE

and (2),

$$v_X(t) = v(t) \cdot \cos\theta \quad (1)$$
$$v_Y(t) = v(t) \cdot \sin\theta \quad (2)$$

where $v(t)$ is wind speed [m/s] and θ is wind direction [°].

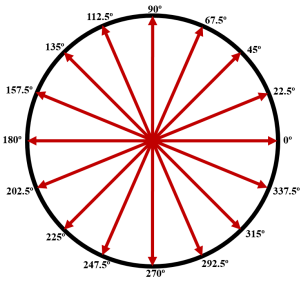

Fig. 1 Definition of wind direction

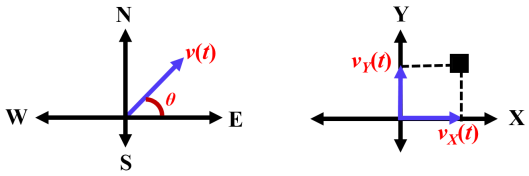

(a) (b)

Fig. 2 Wind speed and direction on coordinate system (a) Vector diagram (b) Definition of component $v(t)$

3.2. Fully connected long short-term memory (FC-LSTM)

LSTM method is powerful and stable with long-term dependencies which have input gate, forget gate, and output gate[8]. In this paper, we use LSTM with fully connected (FC) network which can be called FC-LSTM. The sequence length is set to six which corresponds to one hour. Typically, LSTM unit as shown in Eqs. (3) - (7)[7][8],

$$\boldsymbol{i}_t = \sigma(\boldsymbol{W}_{xi}\cdot\boldsymbol{x}_t+\boldsymbol{W}_{hi}\cdot\boldsymbol{h}_{t-1}+\boldsymbol{W}_{ci}\circ\boldsymbol{c}_{t-1}+b_i) \quad (3)$$
$$\boldsymbol{f}_t = \sigma(\boldsymbol{W}_{xf}\cdot\boldsymbol{x}_t+\boldsymbol{W}_{hf}\cdot\boldsymbol{h}_{t-1}+\boldsymbol{W}_{cf}\circ\boldsymbol{c}_{t-1}+b_f) \quad (4)$$
$$\boldsymbol{c}_t = \boldsymbol{f}_t\circ\boldsymbol{c}_{t-1}+\boldsymbol{i}_t\circ\tanh(\boldsymbol{W}_{xc}\cdot\boldsymbol{x}_t+\boldsymbol{W}_{hc}\cdot\boldsymbol{h}_{t-1}+b_c) \quad (5)$$
$$\boldsymbol{o}_t = \sigma(\boldsymbol{W}_{xo}\cdot\boldsymbol{x}_t+\boldsymbol{W}_{ho}\cdot\boldsymbol{h}_{t-1}+\boldsymbol{W}_{co}\circ\boldsymbol{c}_t+b_o) \quad (6)$$
$$\boldsymbol{h}_t = \boldsymbol{o}_t\circ\tanh(\boldsymbol{c}_t) \quad (7)$$

where $\boldsymbol{i}$ is input gate, $\boldsymbol{f}$ is forget gate, $\boldsymbol{o}$ is output gate, $\boldsymbol{c}$ is cell state, $\boldsymbol{h}$ is hidden state, $\boldsymbol{W}$ is weight, σ is activation function, and $\circ$ means hadamard product.

3.3. ConvLSTM

ConvLSTM can extract features using convolutional operation in input-to-state and state-to-state transitions as shown in Fig 3. The feature map of ConvLSTM layer arranged five dimensions: number of sample data, timestep, height, width and channel (N, ts, h, w and c). ConvLSTM layer produces the output shape of ConvLSTM equivalent to input shape.

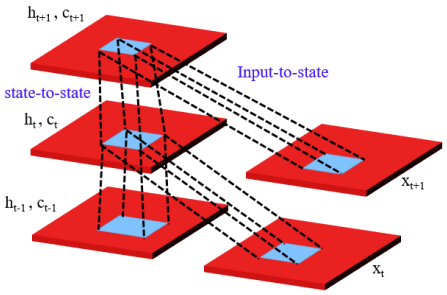

Fig. 3 The core structure of ConvLSTM

ConvLSTM used timestep (sequence length) is set to six which is the same as the sequence length in the FC-LSTM. The matrix product "$\cdot$" in LSTM is replaced convolutional operation "$\star$" in ConvLSTM. The function of ConvLSTM as shown in Eqs. (8) - (12)[7][8][9],

$$\boldsymbol{i}_t = \sigma(\boldsymbol{W}_{xi}\star\boldsymbol{x}_t+\boldsymbol{W}_{hi}\star\boldsymbol{h}_{t-1}+\boldsymbol{W}_{ci}\circ\boldsymbol{c}_{t-1}+b_i) \quad (8)$$
$$\boldsymbol{f}_t = \sigma(\boldsymbol{W}_{xf}\star\boldsymbol{x}_t+\boldsymbol{W}_{hf}\star\boldsymbol{h}_{t-1}+\boldsymbol{W}_{cf}\circ\boldsymbol{c}_{t-1}+b_f) \quad (9)$$
$$\boldsymbol{c}_t = \boldsymbol{f}_t\circ\boldsymbol{c}_{t-1}+\boldsymbol{i}_t\circ\tanh(\boldsymbol{W}_{xc}\star\boldsymbol{x}_t+\boldsymbol{W}_{hc}\star\boldsymbol{h}_{t-1}+b_c) \quad (10)$$
$$\boldsymbol{o}_t = \sigma(\boldsymbol{W}_{xo}\star\boldsymbol{x}_t+\boldsymbol{W}_{ho}\star\boldsymbol{h}_{t-1}+\boldsymbol{W}_{co}\circ\boldsymbol{c}_t+b_o) \quad (11)$$
$$\boldsymbol{h}_t = \boldsymbol{o}_t\circ\tanh(\boldsymbol{c}_t) \quad (12)$$

3.4. Network architecture

We propose a prediction system using an encoding and forecasting network with ConvLSTM. The encoding-forecasting network with ConvLSTM was proposed for precipitation nowcasting and performs good accuracy[8]. In addition, we developed two prediction systems for comparison which are consisted of stacked ConvLSTM and an encoder-decoder network with ConvLSTM.

3.4.1. Stacked ConvLSTM

The network architecture of stacked ConvLSTM is shown in Fig. 4. This network consists of four ConvLSTM2D, four batch normalization and one convolutional3D (Conv3D) layers[10]. The kernel size of ConvLSTM and Conv layers are set to five.

The channel size of convLSTM2D is eight. The last layer of the network is the Conv3D layer for performs sequence to sequence mapping. In the Conv3D layer, channel size is set to one to generate prediction outputs.

3.4.2. Encoder-decoder network with ConvLSTM

The network architecture of encoder-decoder network with ConvLSTM is shown in Fig. 5. This network consists of two parts of encoder and decoder networks[11]. Encoder network consists of three ConvLSTM2D, three batch normalization, and three maxpooling3D layers. Decoder network consists of three deconvolutional3D (Deconv3D), three upsampling3D, and two batch normalization layers.

In the encoder network, the height and width of the feature maps downsampled by ConvLSTM and maxpooling layers. The feature maps are upsampled height and width direction by Deconv and upsampling layers in the decoder network. The kernel size of ConvLSTM2D and

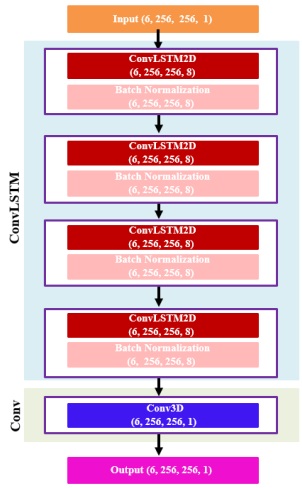

Fig. 4 Network architecture of stacked ConvLSTM

Deconv3D are five. The channel sizes of ConvLSTM2D and Deconv3D are eight. In the decoder network, we use Deconv3D for performing sequence to sequence mapping. The channel size of last layer in decoder network is one to generate the final prediction.

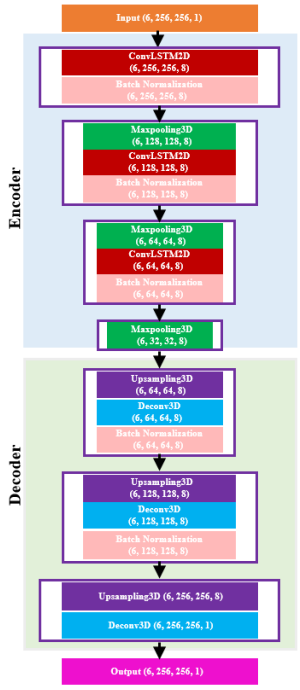

Fig. 5 Network architecture of encoder-decoder network with ConvLSTM

3.4.3. Encoding-forecasting network with ConvLSTM

The network architecture of encoding-forecasting network with ConvLSTM illustrated in Fig. 6 which consists encoding and forecasting networks[8][9]. The encoding network consists of a Conv3D, a maxpooling3D, and three ConvLSTM2D layers. The forecasting network consists of three ConvLSTM2D, a upsampling3D, and a Deconv3D layers. The channel sizes of ConvLSTM2D and Conv3D are eight and four. The kernel size of ConvLSTM, Conv and Deconv layers are set to five.

The feature maps are downsampled for height and width direction by Conv and maxpooling layers in the encoding network. In the forecasting network, the height and width of the feature maps upsampled by Deconv and upsampling layers. The fore input in forecasting network is needed due to the succeeding value of the forecast. Zero arrays are input as the fore input to forecasting network.

The last state of ConvLSTM layer in encoding network after inputting sequence data are copied to the state of the ConvLSTM layer in the forecasting network as shown in Fig. 6. Each network is formed by stacking three layers of ConvLSTM2D. The final prediction in the forecasting network generated one convolutional layer and concatenate all of the states in the forecasting network for getting prediction outputs.

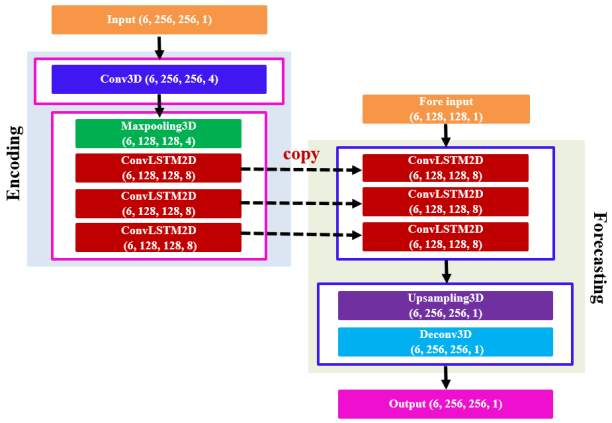

Fig. 6 Network architecture of encoding-forecasting network with ConvLSTM

3.5. Learning parameters

Learning parameters of prediction systems are shown in Table 1. The prediction systems use root mean square propagation (RMSProp) optimizer which utilizing the parameter of learning rate (lr) and rho (ρ). The prediction systems use Leaky rectified linear unit (Leaky ReLU) as activation function. Each network is trained and validated 10 epochs using training and validation dataset.

Table 1 Learning parameters

Parameter	Data		
Optimizer	RMSProp	lr	0.001
		ρ	0.9
Activation function	Leaky ReLU		
Epoch	10		
Batch size	4		

The performance of proposed prediction systems are evaluated based on root mean square error (RMSE) as follows,

$$RMSE = \sqrt{\frac{1}{N}\sum_{q=1}^{N}(y_q - \hat{y}_q)^2} \quad (13)$$

where y_q is observed data, $\hat{y}_q$ is predicted data, and N is sample data.

3.6. Datasets

Wind speed and direction data got from AMeDAS are converted to $v_X(t)$ and $v_Y(t)$ using Eqs. (1) and (2) as shown in Fig. 2(b) and rotated clockwise by 90°. The test data is divided into four seasons. From training dataset, the maximum of wind speed is 20 m/s so that we designed the plotting scale adjusted the size of input images and python imaging library (PIL) as shown in Eqs. (14) - (15),

$$p_X = \left(\frac{128}{20} \cdot v_X\right) + 128 \tag{14}$$

$$p_Y = 128 - \left(\frac{128}{20} \cdot v_Y\right) \tag{15}$$

where p_X is the position wind data of X-axis, p_Y is the position of wind data of Y-axis, and the value of $\left(\frac{128}{20}\right)$ is conversion factor coefficients of the pixel from wind data.

In order to express histories of wind speed and direction using six points at time t, t-1, t-2, t-3, t-4, and t-5 that plotted and connected by the line which is described one hour data as shown in Fig. 7. The black point of current data is bigger than the past data for it differs. The size of input and output images are set to 256 × 256 pixel. The dataset of period using training, validation and test data as shown in Table 2.

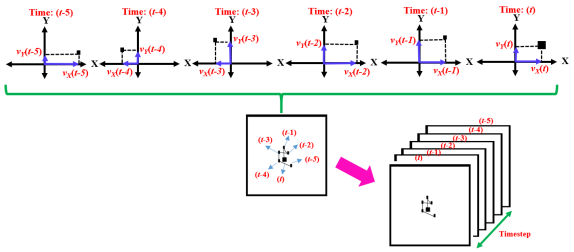

Fig. 7 Process of input image generation

Table 2 Dataset of period

Dataset	Period	
Training	Dec. 2014 - Nov. 2015	
Validation	Dec. 2015 - Feb. 2016	
Test	spring	Mar. - May 2016
	summer	Jun. - Aug. 2016
	autumn	Sep. - Nov. 2016
	winter	Dec. 2016 - Feb. 2017

4. PREDICTION RESULTS

The prediction result is extracted from predicted image as gravity center position of the largest pixel cluster with value zero. The position of prediction result is converted to $\hat{v}_X(t)$ and $\hat{v}_Y(t)$ by substracting the center position of image (128, 128) which are calculated $\hat{p}_X$ and $\hat{p}_Y$ by Eqs. (16) and (17),

$$\hat{v}_X(t) = \left(\frac{20}{128}\right) \cdot (\hat{p}_X - 128) \tag{16}$$

$$\hat{v}_Y(t) = \left(\frac{20}{128}\right) \cdot (128 - \hat{p}_Y) \tag{17}$$

where $\hat{v}_X(t)$ and $\hat{v}_Y(t)$ are X and Y components of predicted wind speed vector $\hat{v}(t)$ [m/s], $\hat{p}_X$ is center position of predicted image in X-axis, and $\hat{p}_Y$ is center position of predicted image in Y-axis. The prediction result of wind speed and direction are calculated by Eqs. (18) and (19),

$$\hat{\theta} = \tan^{-1}\left(\frac{\hat{v}_Y(t)}{\hat{v}_X(t)}\right) \tag{18}$$

$$\hat{v}(t) = \sqrt{\hat{v}_X^2(t) + \hat{v}_Y^2(t)} \tag{19}$$

where $\hat{v}(t)$ is predicted wind speed [m/s], and $\hat{\theta}$ is predicted wind direction [°].

The target is a image one hour ahead and Figs. 8 - 11 show the predicted and observed wind speed and direction for one day of each season: spring (Mar. 8, 2016), summer (Jun. 8, 2016), autumn (Sep. 8, 2016) and winter (Dec. 8, 2016). From Figs. 8 - 11, predicted wind speed and direction by using encoding-forecasting network with ConvLSTM are better than other systems and approaches the observed data. In the graph of wind direction in Figs. 8 - 11, the direction of 180° = -180°.

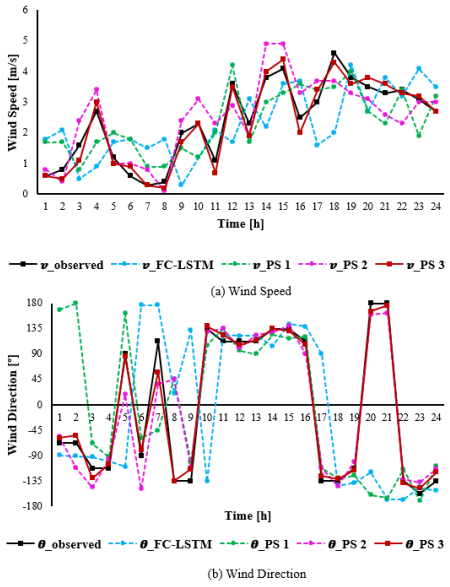

Fig. 8 The result of one day wind speed and direction in spring (Mar. 8, 2016)

Figures 12 and 13 show RMSE of wind speed and direction for each month of Mar. 2016 - Feb. 2017. From Figs. 8 - 13, PS1 is prediction system of stacked ConvLSTM, PS2 is prediction system of encoder-decoder network with ConvLSTM and PS3 is prediction system of encoding-forecasting network with ConvLSTM. Moreover, RMSE of wind speed and direction for each season of Mar. 2016 - Feb. 2017 as shown in Table 3.

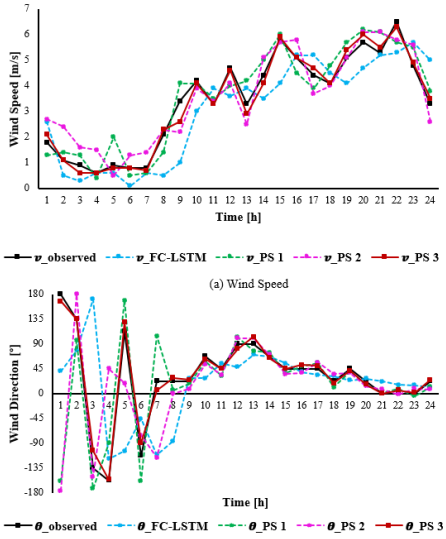

Fig. 9 The result of one day wind speed and direction in summer (Jun. 8, 2016)

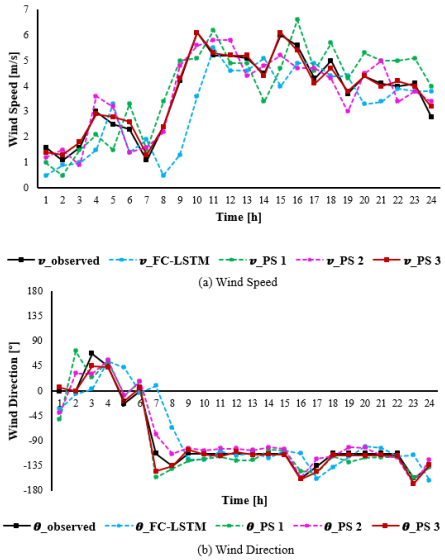

Fig. 10 The result of one day wind speed and direction in autumn (Sep. 8, 2016)

The encoding-forecasting network with ConvLSTM performs the highest prediction accuracy for wind speed and direction among all prediction systems in all seasons as shown in Table 3. Figs. 12 and 13 show that the prediction accuracy of the encoding-forecasting network with ConvLSTM is the highest in most months, regardless the season. This indicates that encoding-forecasting network with ConvLSTM is the best method.

On the other hand, the FC-LSTM performs the lowest accuracy for both wind speed and direction. From Figs. 8 - 11, there are prediction delays for the rapid change of wind speed and direction for the FC-LSTM. Similarly, there are some delays in the wind speed prediction for stacked ConvLSTM although it improved compare to the FC-LSTM. Therefore, it is confirmed that the encoder-decoder network with ConvLSTM and the

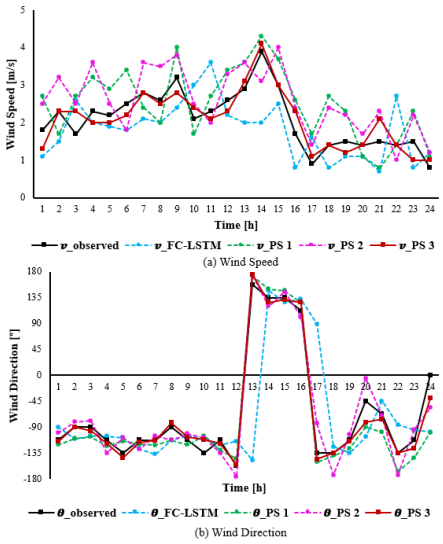

Fig. 11 The result of one day wind speed and direction in winter (Dec. 8, 2016)

encoding-forecasting network with ConvLSTM can extract spatiotemporal features correctly.

The training time of the systems is listed in Table 4. The stacked ConvLSTM is longer training time than FC-LSTM due to this system combined Conv3D layer. The encoder-decoder network with ConvLSTM is longer training time than stacked ConvLSTM due to this system combined three layer Deconv3D.

The encoding-forecasting network with ConvLSTM is shorter training time than stacked ConvLSTM and encoder-decoder network with ConvLSTM caused this system having process copied last state from ConvLSTM layer in encoding network to state ConvLSTM layer in forecasting network and it caused easy to run the program than stacked ConvLSTM and encoder-decoder network with ConvLSTM. The encoding-forecasting network with ConvLSTM is the benchmark method that improved accuracy and effectively needs shorter training time than stacked ConvLSTM and encoder-decoder network with ConvLSTM.

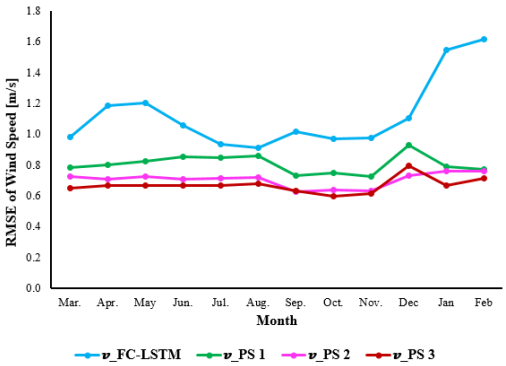

Fig. 12 RMSE of wind speed for each month

Table 3 RMSE of wind speed and direction for all season

Description		RMSE			
		FC-LSTM	stacked ConvLSTM	encoder-decoder network with ConvLSTM	encoding-forecasting network with ConvLSTM
Spring	$v(t)$[m/s]	1.1257	0.8011	0.7191	**0.6588**
	θ [°]	45.3794	35.6979	33.8240	**27.7298**
Summer	$v(t)$[m/s]	0.9666	0.8520	0.7117	**0.6692**
	θ [°]	50.7650	35. 0061	33.9482	**27.5454**
Autumn	$v(t)$[m/s]	0.9854	0.7324	0.6315	**0.6132**
	θ [°]	39.8416	32.6678	31.5565	**25.9453**
Winter	$v(t)$[m/s]	1.4326	0.8331	0.7479	**0.7261**
	θ [°]	36.7751	33.1920	32.9444	**27.8196**
Total	$v(t)$[m/s]	1.1415	0.8050	0.7027	**0.6679**
	θ [°]	43.5648	34.1620	33.0845	**27.2713**

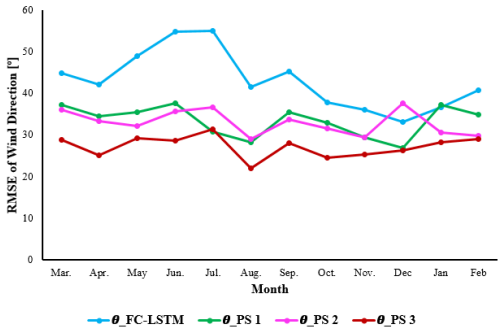

Fig. 13 RMSE of wind direction for each month

Table 4 Training time of all systems

System	Time [min.]
FC-LSTM	10
stacked ConvLSTM	325
encoder-decoder network with ConvLSTM	615
encoding-forecasting network with ConvLSTM	192

5. CONCLUSION

This paper proposed prediction systems of wind speed and direction using encoding-forecasting network with ConvLSTM. The processing data was used in a deep ConvLSTM system. The result of encoding-forecasting network with ConvLSTM is better than other systems. The stacked ConvLSTM, encoder-decoder network with ConvLSTM and encoding-forecasting network with ConvLSTM can be improved prediction accuracy of the FC-LSTM. As the future work, we plan to use the ConvLSTM system in a more complex convolutional likes the number of filters, kernel size and so on for improved accuracy.

REFERENCES

[1] G.V. Laksmi and P.P. Divakar, "Role of renewable energy sources in environmental protection", *Proc. Two-Day International Conference on "Materials for Energy and Environmental Protection"(ICMEEP-18)*, pp. 12–17, 2018.

[2] O. Ellaban, et al., "Renewable energy resources: current status, future prospects and their enabling technology", *Elsevier Journal: Renewable and Sustainable Energy Reviews*, vol. 39, pp. 748–764, 2014.

[3] N. L. Panwar, et al., "Role of renewable energy sources in environmental protection: A review" *Elsevier Journal : Renewable and Sustainable Energy Reviews*., vol. 15, no. 3, pp. 1513–524, 2011.

[4] H. Sori and T. Yasuno , "Correction method for wind speed prediction after a short time using hierarchical neural network', '*Proc. 2008 International Workshop on Nonlinear Circuits and Signal Processing (NSCP'08)*, pp.259–262, 2008.

[5] Y. Miyabe, et al., "Wind speed prediction model using neural networks classified by observed wind speed", *Proc. RISP International Workshop on Nonlinear Circuits, Communications and Signal Processing (NSCP 2015)*, pp. 230–233, 2015.

[6] A.P. Sari, et al., "Prediction model of wind speed and direction using deep neural network", *Journal of Electrical Engineering, Mechatronics and Computer Science*, Vol. 3, no. 1, pp. 1–10, 2020.

[7] S. Agethen and W.H. Hsu, "Deep multi kernel convolutional LSTM Networks and an attention based mechanism for videos", *IEEE Transactions on Multimedia*, Vol. 22, pp. 819–829, 2019.

[8] X. Shi, Z. Chen, et al., "Convolutional LSTM network : A machine learning approach for precipitation nowcasting", *Journal of ArXiv*, Vol. abs/1506.04214, pp. 1–9, 2015.

[9] Y.Y. Hong, et al., "Day-ahead solar irradiation forecasting utilizing gramian angular field and convolutional long short-term memory", *Journal of IEEE access*, Vol. 8, pp. 18741–18753, 2020.

[10] Keras: deep learning for humans, http://www.github.com/keras-team/keras/tree/master/.

[11] A. Kumar, et al., "A recurrent neural network architecture for monocular depth prediction", *IEEE Computer Society Conf. on Computer Vision and Pattern Recognition Workshops*, pp. 396–404, 2018.